Heralded creation of photonic qudits from parametric down-conversion using linear optics

Jun-ichi Yoshikawa,[1,*] Marcel Bergmann,[2] Peter van Loock,[2,†] Maria Fuwa,[1,3] Masanori Okada,[1] Kan Takase,[1] Takeshi Toyama,[1] Kenzo Makino,[1] Shuntaro Takeda,[1] and Akira Furusawa[1,‡]

[1]*Department of Applied Physics, School of Engineering, The University of Tokyo, 7-3-1 Hongo, Bunkyo-ku, Tokyo 113-8656, Japan*

[2]*Institute of Physics, Staudingerweg 7, Johannes Gutenberg-Universität Mainz, 55099 Mainz, Germany*

[3]*Centre of Excellence for Quantum Computation and Communication Technology, Department of Quantum Science, Research School of Physics and Engineering, Building 38a Science Road, The Australian National University, Acton, ACT 2601, Australia*

(Received 24 October 2017; revised manuscript received 13 March 2018; published 14 May 2018)

We propose an experimental scheme to generate, in a heralded fashion, arbitrary quantum superpositions of two-mode optical states with a fixed total photon number n based on weakly squeezed two-mode squeezed state resources (obtained via weak parametric down-conversion), linear optics, and photon detection. Arbitrary d-level (qudit) states can be created this way where $d = n + 1$. Furthermore, we experimentally demonstrate our scheme for $n = 2$. The resulting qutrit states are characterized via optical homodyne tomography. We also discuss possible extensions to more than two modes concluding that, in general, our approach ceases to work in this case. For illustration and with regards to possible applications, we explicitly calculate a few examples such as NOON states and logical qubit states for quantum error correction. In particular, our approach enables one to construct bosonic qubit error-correction codes against amplitude damping (photon loss) with a typical suppression of $\sqrt{n} - 1$ losses and spanned by two logical codewords that each correspond to an n-photon superposition for two bosonic modes.

DOI: 10.1103/PhysRevA.97.053814

I. INTRODUCTION

Photons are an essential ingredient of most protocols for quantum information processing and quantum communication, as they can serve as carriers of "flying quantum information," especially in the form of flying qubits. However, experimentally, deterministic schemes to prepare optical quantum states remain so far within the regime of Gaussian states or classical mixtures of Gaussian states, though, in principle, third-order nonlinear optical effects or interactions with a finite-dimensional system enable one to step out of the Gaussian realm into that of non-Gaussian quantum states [1]. Highly nonclassical, non-Gaussian states of traveling light, pure enough to show negative values in their Wigner functions [2], have been created with probabilistic, heralded schemes [3–12]. These rely on the non-Gaussianity or nonlinearity induced by a photon detection. Since deterministic, 100%-efficient quantum nondemolition measurements of photon numbers [13] are currently unavailable in the optical domain, a photon detection would destroy the measured optical field. Nonetheless, the non-Gaussianity could still be transferred to an outgoing, propagating optical quantum state through quantum correlations.

For the optical resources before the photon detections, two-mode squeezing correlations between signal and idler fields from parametric down-converters are typically utilized. Beyond heralding single photons [3], in previous experiments, an arbitrary superposition of photon-number states up to three photons, i.e., $c_0|0\rangle + c_1|1\rangle + c_2|2\rangle + c_3|3\rangle$ with $c_0, c_1, c_2, c_3 \in \mathbb{C}$, was experimentally generated in a heralded fashion by employing three photon detectors. Before these detections, the idler fields in the heralding lines are combined with auxiliary coherent fields [6,7]. On the other hand, by utilizing the interference of the idler fields in the heralding lines, arbitrary single-photon qubits encoded into two modes, i.e., $c_{10}|10\rangle + c_{01}|01\rangle$ with $c_{10}, c_{01} \in \mathbb{C}$ (so-called dual-rail qubits), were experimentally produced [8,9].

It is then an interesting question whether we can create an arbitrary superposition of photon-number states with, for instance, a total photon number of two distributed in two modes, i.e., $c_{20}|20\rangle + c_{11}|11\rangle + c_{02}|02\rangle$ with $c_{20}, c_{11}, c_{02} \in \mathbb{C}$. This set of quantum states forms a qutrit whose three-dimensional Hilbert space is spanned by the three basis states $\{|20\rangle, |11\rangle, |02\rangle\}$. One can think of this qutrit also as a spin-1 particle with a spin value 1 corresponding to half of the total photon number, $(n_1 + n_2)/2 = n/2 = 1$, and the three possible spin projections corresponding to half of the photon-number differences of the two modes, $(n_1 - n_2)/2 = \{1, 0, -1\}$. More generally, an arbitrary d-level spin particle can be represented by two modes with a spin value corresponding to $(n_1 + n_2)/2 = n/2$ and $d = n + 1$ possible spin projections corresponding to $(n_1 - n_2)/2$ (this is also referred to as the Schwinger representation). In the most general case, a set of number states with a total of n photons distributed in m modes, $\{|n_1, \ldots, n_m\rangle\}$ with $\sum_{k=1}^{m} n_k = n$, spans a d-dimensional Hilbert space where

$$d = \left(\!\!\binom{m}{n}\!\!\right) = \binom{m+n-1}{n} = \frac{(m+n-1)!}{n!\,(m-1)!}. \quad (1)$$

The qutrit above corresponds to the case of $n = 2$ and $m = 2$, which is one special case of the Schwinger representation

*yoshikawa@ap.t.u-tokyo.ac.jp
†loock@uni-mainz.de
‡akiraf@ap.t.u-tokyo.ac.jp

with generally $m = 2$ and arbitrary n. Such quantum states living in a higher-dimensional Hilbert space are important because, for instance, a quantum error-correction code can be constructed by utilizing a certain subspace as the code space. For this purpose, the Hilbert space of the physical system must be big enough such that a logical quantum state can be robustly mapped between code space and error spaces. More specifically, multiphoton states can possibly be tolerant against amplitude damping and, indeed, when qubit information is encoded, for example, as $\alpha[(|40\rangle + |04\rangle)/\sqrt{2}] + \beta\,|22\rangle$, the information does not get lost by a random single-photon annihilation [14].

Here we discuss how to create such superposition states in a heralded scheme, utilizing two-mode squeezed states and linear optics in the heralding idler lines. As a consequence, it is shown that an arbitrary superposition with total photon number n can be, in principle, created for the case of mode number $m = 2$, leading to an arbitrary qudit with $d = n + 1$. However, we also find that our scheme cannot be generally extended to the cases of $m \geqslant 3$. Here we also experimentally demonstrate our scheme for the two-mode qutrit case ($n = 2$ and $m = 2$). Our scheme is directly applicable to the construction of bosonic codes against amplitude damping [14]. The scheme described here can possibly be combined with recent memory schemes [15,16], by which the success event rate may be considerably improved. This paper is organized as follows. In Sec. II, we review how the creation of a heralded single photon is mathematically described, and then we discuss how this can be extended to a single-photon qubit with $n = 1$ and $m = 2$. In Sec. III, we describe the heralded creation of a qutrit for the case of $n = 2$ and $m = 2$, based on the factorization of a corresponding polynomial. In Sec. IV, we present a general extension of the polynomial factorization to the qudit cases of $n \geqslant 3$ and $m = 2$. In Sec. V, we discuss that further extensions of our scheme to $m \geqslant 3$ are, in general, impossible. In Sec. VI, we present a few examples and applications of our qudit generation scheme. In Sec. VII, we present an experimental demonstration of our scheme by using time bins. The density matrices of the heralded states are fully characterized by quantum tomography, employing homodyne detectors for the simultaneous measurements of quadrature values [9]. Further examples are presented in the appendices.

II. HERALDED CREATION OF AN ARBITRARY QUBIT

In a heralded scheme, typically two-mode squeezing by parametric down-conversion is employed with sufficiently weak pumping, where signal and idler photons are probabilistically created in pairs. Mathematically, the initial two-mode squeezed state is expressed as $\sqrt{1-q^2}\sum_{n=0}^{\infty} q^n\,|n\rangle_s\,|n\rangle_i$, where weak pumping corresponds to $q \ll 1$. In the following, we omit the normalization factor $\sqrt{1-q^2}$; however, when the success probability of projecting a two-mode squeezed state onto a desired state is considered, this normalization factor must be taken into account. Then the detection of idler photons means projection onto $\sum_{n=1}^{\infty} |n\rangle_i\,\langle n|$. However, in the case of very weak pumping, higher photon-number detections are unlikely, so we approximate the projection operator by $|1\rangle_i\,\langle 1|$. Alternatively, the detector can be a photon-number-resolving (PNR) detector with high efficiency, in which case

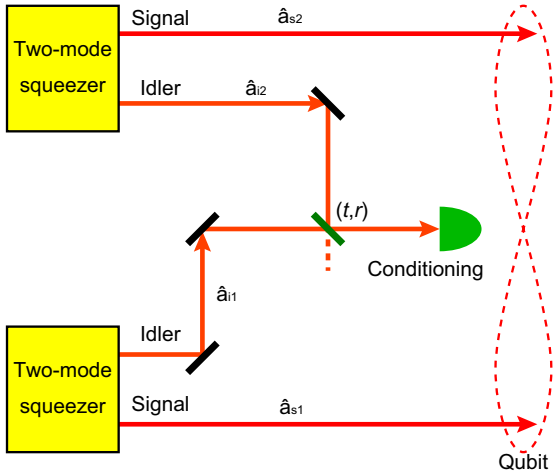

FIG. 1. Scheme for creating a qubit $c_{10}\,|10\rangle + c_{01}\,|01\rangle$.

the projection $|1\rangle_i\,\langle 1|$ is obtained even with strong pumping by discarding the cases of two or more detected idler photons. In addition, since we are not interested in the idler state after the measurement, in the following we express the projection measurement simply by a bra vector, ${}_i\langle 1| = {}_i\langle 0|\,\hat{a}_i$, where $\hat{a}_i$ is the annihilation operator for the idler mode. The process of creating a heralded single photon can then be described by

$$\begin{aligned} &{}_i\langle 1|\sum_{n=0}^{\infty} q^n\,|n\rangle_s\,|n\rangle_i \\ &= {}_i\langle 0|\,\hat{a}_i\sum_{n=0}^{\infty}\frac{q^n}{n!}\hat{a}_s^{\dagger n}\hat{a}_i^{\dagger n}\,|0\rangle_s\,|0\rangle_i \\ &= q\hat{a}_s^{\dagger}\,|0\rangle_s = q\,|1\rangle_s\,. \end{aligned} \tag{2}$$

Here, we intentionally introduced the annihilation and creation operators $\hat{a}$ and $\hat{a}^{\dagger}$, with the prospect of later use. Their commutation relation is $[\hat{a}_j,\hat{a}_k^{\dagger}] = \delta_{jk}$. The error rate due to the approximation of $\sum_{n=1}^{\infty}|n\rangle_i\,\langle n|$ by $|1\rangle_i\,\langle 1|$ based on weak pumping is of the order of q^2. These higher-photon-number components turn the signal state into a mixed state.

An arbitrary single-photon (dual-rail) qubit $c_{10}\,|10\rangle + c_{01}\,|01\rangle$ can be created by combining two idler fields from two parametric down-converters at a beam splitter before the photon detection [8,9]. This basically means adjusting the erasure of which-path information [17]. The scheme is illustrated in Fig. 1. Note that the actual experimental demonstration was for a time-bin qubit [8,9], in which case "two idler fields from two parametric down-converters" actually means idler fields generated at (sufficiently) different times by a single parametric down-converter. The scheme starts with

$$\sum_{n_1=0}^{\infty} q^{n_1}\,|n_1\rangle_{s1}\,|n_1\rangle_{i1}\otimes\sum_{n_2=0}^{\infty} q^{n_2}\,|n_2\rangle_{s2}\,|n_2\rangle_{i2}\,, \tag{3}$$

and the projection by a photon detection at one output port of the beam splitter is expressed by ${}_{i1}\langle 1|\,{}_{i2}\langle 0|\,\hat{U}_{i1,i2}(t,r)$, under the approximation of neglecting the possibility of higher excitations irrelevant to the photon detection (i.e., neglecting orders $\sim q^2$). Alternatively, in the case of strong pumping with a PNR detector, the projection by ${}_{i2}\langle 0|$ has to be confirmed

by another photon detector. Here, $\hat{U}_{k,\ell}(t,r)$ is a unitary operator representing a beam-splitter transformation on modes k and ℓ with a transmission coefficient $t \in \mathbb{C}$ and a reflection coefficient $r \in \mathbb{C}$, satisfying $|t|^2 + |r|^2 = 1$. It transforms the annihilation operators as

$$\hat{U}^\dagger_{k,\ell}(t,r)\hat{a}_k\hat{U}_{k,\ell}(t,r) = t\hat{a}_k + r\hat{a}_\ell, \tag{4a}$$

$$\hat{U}^\dagger_{k,\ell}(t,r)\hat{a}_\ell\hat{U}_{k,\ell}(t,r) = -r^*\hat{a}_k + t^*\hat{a}_\ell, \tag{4b}$$

where the superscript $*$ denotes complex conjugate. Then, the projection bra vector is rewritten as

$$\begin{aligned} {}_{i1}\langle 1|\,{}_{i2}\langle 0|\,\hat{U}_{i1,i2}(t,r) &= {}_{i1}\langle 0|\,{}_{i2}\langle 0|\,\hat{a}_{i1}\hat{U}_{i1,i2}(t,r) \\ &= {}_{i1}\langle 0|\,{}_{i2}\langle 0|\,\hat{U}^\dagger_{i1,i2}(t,r)\hat{a}_{i1}\hat{U}_{i1,i2}(t,r) \\ &= {}_{i1}\langle 0|\,{}_{i2}\langle 0|\,(t\hat{a}_{i1} + r\hat{a}_{i2}). \end{aligned} \tag{5}$$

Note that here we utilized that a two-mode vacuum state is not changed by a beam splitter, $\hat{U}_{i1,i2}(t,r)\,|0\rangle_{i1}\,|0\rangle_{i2} = |0\rangle_{i1}\,|0\rangle_{i2}$. The resulting state after the projection is

$$\begin{aligned} &{}_{i1}\langle 1|\,{}_{i2}\langle 0|\,\hat{U}_{i1,i2}(t,r)\sum_{n_1,n_2=0}^{\infty} q^{n_1}q^{n_2}\,|n_1\rangle_{s1}\,|n_1\rangle_{i1}\,|n_2\rangle_{s2}\,|n_2\rangle_{i2} \\ &= {}_{i1}\langle 0|\,{}_{i2}\langle 0|\,(t\hat{a}_{i1} + r\hat{a}_{i2}) \\ &\quad\times\sum_{n_1,n_2=0}^{\infty} q^{n_1}q^{n_2}\frac{\hat{a}^{\dagger n_1}_{s1}\hat{a}^{\dagger n_1}_{i1}}{n_1!}\frac{\hat{a}^{\dagger n_2}_{s2}\hat{a}^{\dagger n_2}_{i2}}{n_2!}\,|0\rangle_{s1}\,|0\rangle_{i1}\,|0\rangle_{s2}\,|0\rangle_{i2} \\ &= q(t\hat{a}^\dagger_{s1} + r\hat{a}^\dagger_{s2})\,|0\rangle_{s1}\,|0\rangle_{s2} \\ &= q(t\,|1\rangle_{s1}\,|0\rangle_{s2} + r\,|0\rangle_{s1}\,|1\rangle_{s2}), \end{aligned} \tag{6}$$

up to the normalization factor. Since the coefficients t and r can be arbitrarily determined under the constraint $|t|^2 + |r|^2 = 1$ via the beam-splitting ratio and a phase shift before the interference, an arbitrary qubit $c_{10}\,|1\rangle_{s1}\,|0\rangle_{s2} + c_{01}\,|0\rangle_{s1}\,|1\rangle_{s2}$ is probabilistically created with this scheme. Because a photon detection is phase insensitive, a phase shift after the interference is meaningless and thus only a phase shift before the interference at the beam splitter can change the argument of the complex numbers t or r. For a projection onto ${}_{i1}\langle 0|\,{}_{i2}\langle 1|\,\hat{U}_{i1,i2}(t,r)$ (corresponding to the detection of one photon in the other beam-splitter output port), it is easy to see that a similar calculation leads to the orthogonal dual-rail qubit state in the signal output modes, $q(-r^*\,|1\rangle_{s1}\,|0\rangle_{s2} + t^*\,|0\rangle_{s1}\,|1\rangle_{s2})$. Note that for the special case of $t = r = 1/\sqrt{2}$, the scheme resembles the entanglement distribution in the quantum repeater protocol of Ref. [18] with the two signal modes distributed among two repeater stations.

III. HERALDED CREATION OF AN ARBITRARY QUTRIT

Let us now consider the case of a qutrit with a total photon number of $n = 2$ in $m = 2$ modes, i.e.,

$$\begin{aligned} &c_{20}\,|20\rangle_{1,2} + c_{11}\,|11\rangle_{1,2} + c_{02}\,|02\rangle_{1,2} \\ &= \left(\frac{c_{20}}{\sqrt{2}}\hat{a}^{\dagger 2}_1 + c_{11}\hat{a}^\dagger_1\hat{a}^\dagger_2 + \frac{c_{02}}{\sqrt{2}}\hat{a}^{\dagger 2}_2\right)|00\rangle_{1,2}\,. \end{aligned} \tag{7}$$

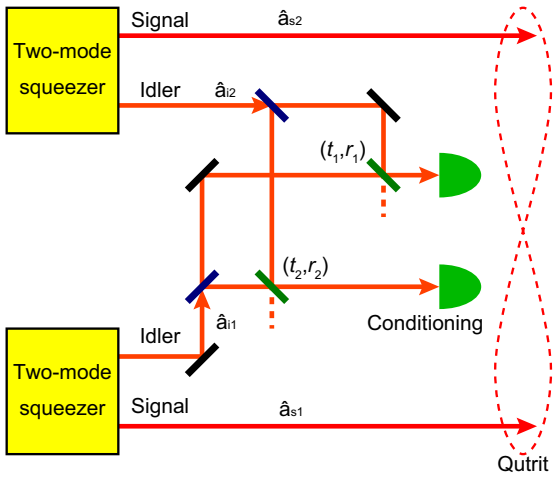

FIG. 2. Scheme for creating a qutrit $c_{20}\,|20\rangle + c_{11}\,|11\rangle + c_{02}\,|02\rangle$.

The crucial observation is the following decomposition:

$$\begin{aligned} &c_{20}\hat{a}^{\dagger 2}_1 + \sqrt{2}c_{11}\hat{a}^\dagger_1\hat{a}^\dagger_2 + c_{02}\hat{a}^{\dagger 2}_2 \\ &\quad= (d_{11}\hat{a}^\dagger_1 + d_{12}\hat{a}^\dagger_2)(d_{21}\hat{a}^\dagger_1 + d_{22}\hat{a}^\dagger_2), \end{aligned} \tag{8}$$

where $c_{20},c_{11},c_{02} \in \mathbb{C}$, $d_{11},d_{12},d_{21},d_{22} \in \mathbb{C}$. Since all the creation operators commute with each other, this decomposition corresponds to the problem of factorizing polynomials with complex coefficients,

$$c_{20}z^2 + \sqrt{2}c_{11}z + c_{02} = (d_{11}z + d_{12})(d_{21}z + d_{22}). \tag{9}$$

However, this factorization is always possible from the fundamental theorem of algebra. The answer of $az^2 + bz + c = 0$ is $z = (-b \pm \sqrt{b^2 - 4ac})/2a$ when $a \neq 0$, where $\sqrt{|u|e^{i\theta}}$ is either $\sqrt{|u|}e^{i\theta/2}$ or $\sqrt{|u|}e^{i\pi+i\theta/2}$.

For implementing the product of two first-order terms $d_{11}\hat{a}^\dagger_1 + d_{12}\hat{a}^\dagger_2$ and $d_{21}\hat{a}^\dagger_1 + d_{22}\hat{a}^\dagger_2$, the simplest way is to split each of the two idler modes into two by a beam splitter. The scheme is depicted in Fig. 2. We introduce two ancilla modes in a vacuum state $|0\rangle_{a1}\,|0\rangle_{a2}$, which enter the unused ports of the beam splitters. Then we combine the two split idler modes at two beam splitters with different transmission and reflection coefficients, (t_1,r_1) and (t_2,r_2). More specifically, here we take the beam-splitter operation as

$$\begin{aligned} &\hat{U}_{i1,i2}(t_1,r_1)\hat{U}_{a1,a2}(t_2,r_2) \\ &\quad\times\hat{U}_{i1,a1}\left(\frac{1}{\sqrt{2}},-\frac{1}{\sqrt{2}}\right)\hat{U}_{i2,a2}\left(\frac{1}{\sqrt{2}},-\frac{1}{\sqrt{2}}\right), \end{aligned} \tag{10}$$

followed by the projection ${}_{i1,i2,a1,a2}\langle 1,0,1,0|$.

Eventually, the two-mode signal state after the projection becomes

$$
\begin{aligned}
&{}_{i1,i2,a1,a2}\langle 1,0,1,0|\,\hat{U}_{i1,i2}(t_1,r_1)\hat{U}_{a1,a2}(t_2,r_2)\hat{U}_{i1,a1}\left(\frac{1}{\sqrt{2}},-\frac{1}{\sqrt{2}}\right)\\
&\quad\times\hat{U}_{i2,a2}\left(\frac{1}{\sqrt{2}},-\frac{1}{\sqrt{2}}\right)\sum_{n_1,n_2=0}^{\infty}q^{n_1}q^{n_2}\,|n_1,n_1,n_2,n_2\rangle_{s1,i1,s2,i2}\,|0,0\rangle_{a1,a2}\\
&=\,{}_{i1,i2,a1,a2}\langle 0,0,0,0|\,(t_1\hat{a}_{i1}+r_1\hat{a}_{i2})(t_2\hat{a}_{a1}+r_2\hat{a}_{a2})\hat{U}_{i1,a1}\left(\frac{1}{\sqrt{2}},-\frac{1}{\sqrt{2}}\right)\hat{U}_{i2,a2}\left(\frac{1}{\sqrt{2}},-\frac{1}{\sqrt{2}}\right)\\
&\quad\times\sum_{n_1,n_2=0}^{\infty}q^{n_1}q^{n_2}\,|n_1,n_1,n_2,n_2\rangle_{s1,i1,s2,i2}\,|0,0\rangle_{a1,a2}\\
&=\,{}_{i1,i2,a1,a2}\langle 0,0,0,0|\left[t_1\left(\frac{\hat{a}_{i1}-\hat{a}_{a1}}{\sqrt{2}}\right)+r_1\left(\frac{\hat{a}_{i2}-\hat{a}_{a2}}{\sqrt{2}}\right)\right]\left[t_2\left(\frac{\hat{a}_{i1}+\hat{a}_{a1}}{\sqrt{2}}\right)+r_2\left(\frac{\hat{a}_{i2}+\hat{a}_{a2}}{\sqrt{2}}\right)\right]\\
&\quad\times\sum_{n_1,n_2=0}^{\infty}q^{n_1}q^{n_2}\frac{\hat{a}_{s1}^{\dagger n_1}\hat{a}_{i1}^{\dagger n_1}}{n_1!}\frac{\hat{a}_{s2}^{\dagger n_2}\hat{a}_{i2}^{\dagger n_2}}{n_2!}\,|0,0,0,0,0,0\rangle_{s1,i1,s2,i2,a1,a2}\\
&=\frac{q^2}{2}\left(t_1t_2\hat{a}_{s1}^{\dagger 2}+t_1r_2\hat{a}_{s1}^{\dagger}\hat{a}_{s2}^{\dagger}+r_1t_2\hat{a}_{s2}^{\dagger}\hat{a}_{s1}^{\dagger}+r_1r_2\hat{a}_{s2}^{\dagger 2}\right)|0,0\rangle_{s1,s2}\\
&=\frac{q^2}{2}\left(t_1\hat{a}_{s1}^{\dagger}+r_1\hat{a}_{s2}^{\dagger}\right)\left(t_2\hat{a}_{s1}^{\dagger}+r_2\hat{a}_{s2}^{\dagger}\right)|0,0\rangle_{s1,s2}\,. \qquad (11)
\end{aligned}
$$

Note that $\langle 0|\,\hat{a}^2\hat{a}^{\dagger 2}\,|0\rangle = 2$ is used in the above calculation. Taking account of the omitted normalization factor $\sqrt{1-q^2}$ for each of the two-mode squeezed states, and of a *bias factor* discussed below, the success probability of projecting the two-mode squeezed states into a desired qutrit state is in the range from $q^4(1-q^2)^2/4$ to $q^4(1-q^2)^2/2$, depending on the target qutrit state. Note that in the case of a qubit in Eq. (6), the success probability $q^2(1-q^2)^2$ is equal for all states.

A. Interpretation of the bias factor

The first excitation $\hat{b}_2^{\dagger} := t_2\hat{a}_1^{\dagger}+r_2\hat{a}_2^{\dagger}$ can be decomposed into a part parallel to the second excitation $\hat{b}_1^{\dagger} := t_1\hat{a}_1^{\dagger}+r_1\hat{a}_2^{\dagger}$ and an orthogonal part $\hat{b}_{1\perp}^{\dagger} := -r_1\hat{a}_1^{\dagger}+t_1\hat{a}_2^{\dagger}$ as

$$\hat{b}_2^{\dagger} = c_{\parallel}\hat{b}_1^{\dagger}+c_{\perp}\hat{b}_{1\perp}^{\dagger}. \qquad (12)$$

However, the parallel part has a twice as large contribution as the orthogonal part,

$$
\begin{aligned}
\hat{b}_1^{\dagger}\hat{b}_2^{\dagger}\,|0,0\rangle_{\hat{b}_1,\hat{b}_{1\perp}} &= \hat{b}_1^{\dagger}(c_{\parallel}\hat{b}_1^{\dagger}+c_{\perp}\hat{b}_{1\perp}^{\dagger})\,|0,0\rangle_{\hat{b}_1,\hat{b}_{1\perp}}\\
&= \sqrt{2}c_{\parallel}\,|2,0\rangle_{\hat{b}_1,\hat{b}_{1\perp}}+c_{\perp}\,|1,1\rangle_{\hat{b}_1,\hat{b}_{1\perp}}, \qquad (13)
\end{aligned}
$$

where the two-mode representation is appropriately chosen so that $\hat{b}_1^{\dagger}\,|0,0\rangle_{\hat{b}_1,\hat{b}_{1\perp}} = |1,0\rangle_{\hat{b}_1,\hat{b}_{1\perp}}$ and $\hat{b}_{1\perp}^{\dagger}\,|0,0\rangle_{\hat{b}_1,\hat{b}_{1\perp}} = |0,1\rangle_{\hat{b}_1,\hat{b}_{1\perp}}$.

This "bias" is explained as follows. When $\hat{b}_2^{\dagger}$ is orthogonal to $\hat{b}_1^{\dagger}$, the photon that heralds $\hat{b}_1^{\dagger}$ must, after the beam-splitter network, go to the detector ${}_{i1}\langle 1|$, while the photon that heralds $\hat{b}_2^{\dagger}$ must go to the detector ${}_{a1}\langle 1|$. On the other hand, when $\hat{b}_2^{\dagger}$ is parallel to $\hat{b}_1^{\dagger}$, the photon that heralds $\hat{b}_1^{\dagger}$ may go to either of ${}_{i1}\langle 1|$ and ${}_{a1}\langle 1|$, while the photon that heralds $\hat{b}_2^{\dagger}$ must go to the other detector. This freedom of swapping photons increases the contribution of parallel components. Although the initial two-mode squeezed state $\sum_{n_1,n_2=0}^{\infty}q^{n_1}q^{n_2}\,|n_1,n_1,n_2,n_2\rangle_{s1,i1,s2,i2}$ equally contains all the two-photon signal state $c_{2,0}\,|2,0\rangle_{s1,s2}+c_{1,1}\,|1,1\rangle_{s1,s2}+c_{0,2}\,|0,2\rangle_{s1,s2}$ with the probability density $O(q^4)$, $\hat{b}_1^{\dagger 2}$ is twice as likely to be heralded than $\hat{b}_1^{\dagger}\hat{b}_{1\perp}^{\dagger}$.

This observation is naturally extended to the case of general total photon numbers n, which is described in Sec. IV, in which case $\hat{b}_1^{\dagger n-k}\hat{b}_{1\perp}^{\dagger k}$ has a contribution proportional to $(n-k)!k!$.

IV. HERALDED CREATION OF AN ARBITRARY QUDIT

The fundamental theorem of algebra says that an arbitrary nonconstant single-variable polynomial with complex coefficients has at least one complex root. From this, it can be derived that the decomposition into first-order terms,

$$
\begin{aligned}
&c_nz^n+c_{n-1}z^{n-1}+\cdots+c_1z+c_0\\
&\quad=c_n(z+d_1)(z+d_2)\cdots(z+d_n), \qquad (14)
\end{aligned}
$$

is always possible when $c_n\neq 0$.

Therefore, an arbitrary superposition state can be, in principle, decomposed as a product of first-order creation terms on a vacuum state,

$$
\begin{aligned}
&\sum_{k=0}^{n}c_{(n-k)k}\,|n-k\rangle_1\,|k\rangle_2\\
&\quad=\sum_{k=0}^{n}\frac{c_{(n-k)k}}{\sqrt{(n-k)!k!}}\hat{a}_1^{\dagger n-k}\hat{a}_2^{\dagger k}\,|0\rangle_1\,|0\rangle_2\\
&\quad=\left[\prod_{k=0}^{n}(d_{k,1}\hat{a}_1^{\dagger}+d_{k,2}\hat{a}_2^{\dagger})\right]|0\rangle_1\,|0\rangle_2\,. \qquad (15)
\end{aligned}
$$

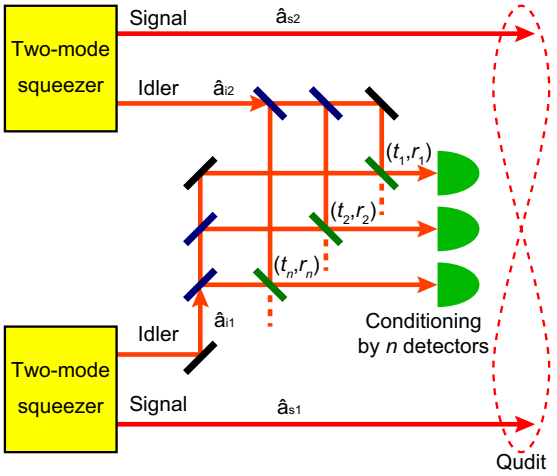

FIG. 3. Scheme for creating a qudit $\sum_{k=0}^{n} c_{(n-k)k}\,|n-k\rangle\,|k\rangle$, where the dimension is $d=n+1$. The number of the conditioning detectors corresponds to the total photon number n. The figure, as an example, is for $n=3$.

This is created via a heralded scheme depicted in Fig. 3, which is a natural extension of the two-photon qutrit case in Sec. III. We first equally split each of the two idler modes into n modes by a series of beam splitters. Mathematically, for each idler mode $k=1,2$, we introduce $n-1$ ancilla vacuum modes, and we combine them at a series of beam splitters, which is, for instance, described by

$$\hat{\mathcal{U}}_k=\hat{U}_{ik,ak1}\left(\frac{1}{\sqrt{2}},-\frac{1}{\sqrt{2}}\right)\hat{U}_{ik,ak2}\left(\sqrt{\frac{2}{3}},-\frac{1}{\sqrt{3}}\right)\cdots\hat{U}_{ik,ak(n-1)}\left(\sqrt{\frac{n-1}{n}},-\frac{1}{\sqrt{n}}\right). \tag{16}$$

This network divides the idler modes with an equal weight,

$$[\hat{\mathcal{U}}_k^\dagger\hat{a}_{ik}\hat{\mathcal{U}}_k,\hat{a}_{ik}^\dagger]=[\hat{\mathcal{U}}_k^\dagger\hat{a}_{ak\ell}\hat{\mathcal{U}}_k,\hat{a}_{ik}^\dagger]=\frac{1}{\sqrt{n}}, \tag{17}$$

for $\ell=1,\ldots,n-1$. Then we combine the two sets of the split idler modes at n beam splitters $\hat{U}_{i1,i2}(t_1,r_1)$, $\hat{U}_{a11,a21}(t_2,r_2),\ldots,\hat{U}_{a1(n-1),a2(n-1)}(t_n,r_n)$, each followed by a photon detection. The whole procedure can be expressed as

$$\begin{aligned}
&{}_{i1,i2,a11,a21,\ldots,a1(n-1),a2(n-1)}\langle 1,0,1,0,\ldots,1,0|\,\hat{U}_{i1,i2}(t_1,r_1)\hat{U}_{a11,a21}(t_2,r_2)\cdots\hat{U}_{a1(n-1),a2(n-1)}(t_n,r_n)\hat{\mathcal{U}}_1\hat{\mathcal{U}}_2\\
&\quad\times\sum_{n_1,n_2=0}^{\infty}q^{n_1}q^{n_2}\,|n_1,n_1,n_2,n_2\rangle_{s1,i1,s2,i2}\,|0,0,\ldots,0,0\rangle_{a11,a21,\ldots,a1(n-1),a2(n-1)}\\
&=\,{}_{i1,i2,a11,a21,\ldots,a1(n-1),a2(n-1)}\langle 0,0,0,0,\ldots,0,0|\,(t_1\hat{\mathcal{U}}_1^\dagger\hat{a}_{i1}\hat{\mathcal{U}}_1+r_1\hat{\mathcal{U}}_2^\dagger\hat{a}_{i2}\hat{\mathcal{U}}_2)(t_2\hat{\mathcal{U}}_1^\dagger\hat{a}_{a11}\hat{\mathcal{U}}_1+r_2\hat{\mathcal{U}}_2^\dagger\hat{a}_{a21}\hat{\mathcal{U}}_2)\cdots\\
&\quad\times(t_n\hat{\mathcal{U}}_1^\dagger\hat{a}_{a1(n-1)}\hat{\mathcal{U}}_1+r_n\hat{\mathcal{U}}_2^\dagger\hat{a}_{a2(n-1)}\hat{\mathcal{U}}_2)\sum_{n_1,n_2=0}^{\infty}q^{n_1}q^{n_2}\frac{\hat{a}_{s1}^{\dagger n_1}\hat{a}_{i1}^{\dagger n_1}}{n_1!}\frac{\hat{a}_{s2}^{\dagger n_2}\hat{a}_{i2}^{\dagger n_2}}{n_2!}\,|0,0,0,0,0,0,\ldots,0,0\rangle_{s1,i1,s2,i2,a11,a21,\ldots,a1(n-1),a2(n-1)}\\
&=\frac{q^n}{n^{n/2}}(t_1\hat{a}_{s1}^\dagger+r_1\hat{a}_{s2}^\dagger)\cdots(t_n\hat{a}_{s1}^\dagger+r_n\hat{a}_{s2}^\dagger)\,|0,0\rangle_{s1,s2}\,.
\end{aligned} \tag{18}$$

Note that $\langle 0|\,\hat{a}^n\hat{a}^{\dagger n}\,|0\rangle=n!$ is used in the above calculation.

Like above, the heralded creation of a qudit with n photons is, in principle, possible based on the decomposition into first-order terms. However, finding the set of decomposition coefficients $\{d_{k\ell}\}$ for a specific case $\{c_{k\ell}\}$ is not an easy problem in general, as well as the factorization of the nth-order polynomial.

V. POSSIBILITY OF FURTHER MULTIMODE EXTENSIONS

So far, we have discussed that an arbitrary superposition state with an arbitrary total photon number n can be, in principle, created with heralded schemes when the number of modes is $m=2$. Similarly, we may consider an extension to a general number of modes m as

$$\sum_{n_1+\cdots+n_m=n}c_{n_1,\ldots,n_m}\,|n_1,\ldots,n_m\rangle_{1,\ldots,m}\,. \tag{19}$$

In this general case, we have to consider the factorization of a polynomial with $m-1$ variables,

$$\sum_{n_1+\cdots+n_m=n}\frac{c_{n_1,\ldots,n_m}}{\sqrt{n_1!\ldots n_m!}}z_1^{n_1}\cdots z_{m-1}^{n_{m-1}}. \tag{20}$$

In the case where a factorization into first-order terms $(\sum_{k=1}^{m-1}d_kz_k)+d_m$ is possible, the corresponding state can again be created in a similar manner by utilizing beam-splitter networks before heralding photon detections.

However, it may not be possible to factorize polynomials when they contain more than two variables. Therefore, the cases with more than three modes $m\geqslant 3$ are an open question, except for the trivial case of a total photon number $n\leqslant 1$. In fact, the insufficient degrees of freedom imply the requirement of a totally different scheme instead of the factorization into first-order terms. For instance, for the simplest case of $n=2$ and $m=3$, the polynomial to be factorized (absorbing the

factors of $1/\sqrt{n_1!n_2!n_3!}$ into the coefficients c_{n_1,n_2,n_3}) is

$$c_{2,0,0}z_1^2 + c_{1,1,0}z_1z_2 + c_{0,2,0}z_2^2 + c_{1,0,1}z_1 + c_{0,1,1}z_2 + c_{0,0,2}, \tag{21}$$

while that after the factorization is

$$c_{0,0,2}(1 + d_{1,1}z_1 + d_{1,2}z_2)(1 + d_{2,1}z_1 + d_{2,2}z_2). \tag{22}$$

Obviously, the degree of freedom after the factorization is not sufficient to cover all the second-order polynomials.

Similarly, we can consider the extension to an arbitrary superposition state containing no more than n photons in total, distributed in m modes,

$$\sum_{n_1+\cdots+n_m\leqslant n} c_{n_1,\ldots,n_m}\,|n_1,\ldots,n_m\rangle_{1,\ldots,m}\,. \tag{23}$$

In this case, the desired decomposition is

$$\sum_{n_1+\cdots+n_m\leqslant n} \frac{c_{n_1,\ldots,n_m}}{\sqrt{n_1\ldots n_m k!}}\hat{a}_1^{\dagger n_1}\ldots\hat{a}_m^{\dagger n_m} = \prod_{k=0}^{n}(d_{k,1}\hat{a}_1^\dagger + \cdots + d_{k,m}\hat{a}_m^\dagger + d_{k,m+1}). \tag{24}$$

If the above decomposition is possible, each of the single excitations $d_{k,1}\hat{a}_1^\dagger + \cdots + d_{k,m}\hat{a}_m^\dagger + d_{k,m+1}$ is, in principle, possible since the addition of a zeroth-order term $d_{k,m+1}$ to first-order terms $d_{k,1}\hat{a}_1^\dagger + \cdots + d_{k,m}\hat{a}_m^\dagger$ is possible by a small coherent displacement of the corresponding idler mode in phase space, $\hat{a}_i \to \hat{a}_i + \epsilon_i$, before the photon detection [4–6]. The corresponding polynomial to be factorized becomes

$$\sum_{n_1+\cdots+n_m\leqslant n} \frac{c_{n_1,\ldots,n_m}}{\sqrt{n_1!\ldots n_m!}}z_1^{n_1}\ldots z_m^{n_1}. \tag{25}$$

The polynomial of Eq. (20) is equivalent to that of Eq. (25) when m is replaced by $m+1$, and thus the problem of "up to n photons in m modes" is equivalent to that of "total n photons in $m+1$ modes."

VI. EXAMPLES AND APPLICATIONS

A. Error-correction code for loss

An important possible application of our general superposition states is the creation of quantum error-correction codewords and their logical states. Taking advantage of our scheme to prepare multiphoton states, here we consider an error-correction code against amplitude damping. A famous example is a logical qubit defined as

$$|0\rangle_L = \frac{1}{\sqrt{2}}(|40\rangle + |04\rangle), \tag{26a}$$

$$|1\rangle_L = |22\rangle\,. \tag{26b}$$

Then, $|\Psi\rangle = \alpha\,|0\rangle_L + \beta\,|1\rangle_L$ is a good encoding of a qubit against a random one-photon loss [14]. Assuming $\alpha,\beta \neq 0$, the logical qubit state can be expressed in terms of creation operators,

$$\begin{aligned}
&\frac{\alpha}{\sqrt{2}}(|40\rangle + |04\rangle) + \beta\,|22\rangle \\
&= \left[\frac{\alpha}{\sqrt{2}}\left(\frac{a_1^{\dagger 4}}{\sqrt{4!}} + \frac{a_2^{\dagger 4}}{\sqrt{4!}}\right) + \frac{\beta}{2}a_1^{\dagger 2}a_2^{\dagger 2}\right]|00\rangle \\
&= \left(\frac{\alpha}{4\sqrt{3}}a_1^{\dagger 4} + \frac{\alpha}{4\sqrt{3}}a_2^{\dagger 4} + \frac{\beta}{2}a_1^{\dagger 2}a_2^{\dagger 2}\right)|00\rangle \\
&=: p(a_1^\dagger, a_2^\dagger)\,|00\rangle.
\end{aligned} \tag{27}$$

To find the transmittance and the reflection coefficients in Eq. (11), one has to determine the decomposition of $p(a_1^\dagger, a_2^\dagger)$ into linear factors. A short calculation shows

$$\begin{aligned}
p(a_1^\dagger, a_2^\dagger)\,|00\rangle = \frac{\alpha}{4\sqrt{3}}&\left(a_1^\dagger - a_2^\dagger\sqrt{-\frac{\sqrt{3}\beta}{\alpha} + \sqrt{\frac{3\beta^2}{\alpha^2} - 1}}\right) \\
&\times\left(a_1^\dagger - a_2^\dagger\sqrt{-\frac{\sqrt{3}\beta}{\alpha} - \sqrt{\frac{3\beta^2}{\alpha^2} - 1}}\right) \\
&\times\left(a_1^\dagger + a_2^\dagger\sqrt{-\frac{\sqrt{3}\beta}{\alpha} + \sqrt{\frac{3\beta^2}{\alpha^2} - 1}}\right) \\
&\times\left(a_1^\dagger + a_2^\dagger\sqrt{-\frac{\sqrt{3}\beta}{\alpha} - \sqrt{\frac{3\beta^2}{\alpha^2} - 1}}\right)|00\rangle.
\end{aligned} \tag{28}$$

The expression is not yet in the form of the last line of Eq. (11). This is done by rescaling each linear factor to obtain the transmission and reflection coefficients,

$$t_1 = t_3 = \frac{1}{\sqrt{1 + \left|-\frac{\sqrt{3}\beta}{\alpha} + \sqrt{\frac{3\beta^2}{\alpha^2} - 1}\right|^2}}, \tag{29a}$$

$$r_1 = r_3 = \frac{-\frac{\sqrt{3}\beta}{\alpha} + \sqrt{\frac{3\beta^2}{\alpha^2} - 1}}{\sqrt{1 + \left|-\frac{\sqrt{3}\beta}{\alpha} + \sqrt{\frac{3\beta^2}{\alpha^2} - 1}\right|^2}},$$

$$t_2 = t_4 = \frac{1}{\sqrt{1 + \left|\frac{\sqrt{3}\beta}{\alpha} + \sqrt{\frac{3\beta^2}{\alpha^2} - 1}\right|^2}}, \tag{29b}$$

$$r_2 = r_4 = \frac{-\frac{\sqrt{3}\beta}{\alpha} - \sqrt{\frac{3\beta^2}{\alpha^2} - 1}}{\sqrt{1 + \left|\frac{\sqrt{3}\beta}{\alpha} + \sqrt{\frac{3\beta^2}{\alpha^2} - 1}\right|^2}}.$$

The success probability for obtaining the desired heralded state is found to be

$$\begin{aligned}
P_{\rm succ}(\alpha,\beta) = \frac{48}{\alpha^2}\frac{q^8}{256}(1-q^2)^2&\left(1+\left|-\frac{\sqrt{3}\beta}{\alpha}+\sqrt{\frac{3\beta^2}{\alpha^2}-1}\right|^2\right)^{-1} \\
&\times\left(1+\left|\frac{\sqrt{3}\beta}{\alpha}+\sqrt{\frac{3\beta^2}{\alpha^2}-1}\right|^2\right)^{-1}.
\end{aligned} \tag{30}$$

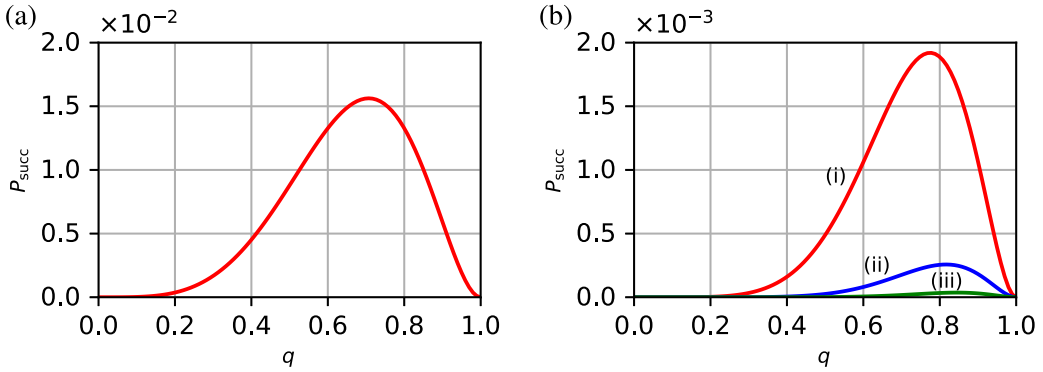

FIG. 4. Success probability for creating $\frac{1}{\sqrt{2}}(|N0\rangle + |0N\rangle)$ for various N in dependence of q (PNRD). Note that the $N = 2$ NOON state can also be directly obtained from two single-photon states using a beam splitter. (a) $N = 2$. (b) (i) $N = 3$, (ii) $N = 4$, (iii) $N = 5$.

Note that the code spanned by the two codewords as given in Eq. (26) can correct losses of up to one photon. In fact, it can easily be seen that the two codewords remain orthogonal after the loss of one photon in either the first or the second mode. Moreover, these two distinct cases lead to logical qubits that live in orthogonal error spaces, $\{|30\rangle, |12\rangle\}$ versus $\{|03\rangle, |21\rangle\}$, respectively. Slightly less simple but also straightforwardly confirmable is that the logical qubit information does not get deformed by the loss of one photon, and so it remains intact in any one of the permitted subspaces. However, once two or more photons get lost, the supposedly different error spaces start overlapping. Thus, the code only works well in the regime of sufficiently small losses. More generally, such a two-mode n-photon loss code can correct up to $\sqrt{n} - 1$ losses and, using our scheme, in principle, any such two-mode code can be experimentally prepared. There are also other loss codes that are based upon a higher number of modes, where we have seen that our generation scheme may no longer be applicable. Nonetheless, a class of such multimode loss codes makes use of an initial supply of so-called NOON states [19]. For this application, but also for other applications in the context of quantum metrology or lithography, the ability to experimentally prepare NOON states is of great interest. We consider this example next.

B. NOON states

A general NOON state is given by

$$\frac{1}{\sqrt{2}}(|N0\rangle + |0N\rangle) = \frac{1}{\sqrt{2}}\left(\frac{a_1^{\dagger N}}{\sqrt{N!}} + \frac{a_2^{\dagger N}}{\sqrt{N!}}\right)|00\rangle. \tag{31}$$

To be able to apply our scheme for their creation, the polynomial

$$p(x,y) = \frac{1}{\sqrt{2N!}}(x^N + y^N) \tag{32}$$

has to be decomposed into linear factors. The decomposition is given by

$$p(x,y) := \frac{1}{\sqrt{2N!}}\prod_{k=0}^{N-1}\left(x - \zeta_{2N}\zeta_N^k y\right), \tag{33}$$

where $\zeta_N = \exp(\frac{2\pi i}{N})$ is the Nth root of unity.

Therefore, one can write

$$\begin{aligned} p(a_1^\dagger, a_2^\dagger)\,|00\rangle &= \frac{1}{\sqrt{2N!}}\prod_{k=0}^{N-1}(a_1^\dagger - \zeta_{2N}\zeta_N^k a_2^\dagger)\,|00\rangle \\ &= \frac{1}{\sqrt{2N!}}\sqrt{2}^N\prod_{k=0}^{N-1}(t_k a_1^\dagger + r_k a_2^\dagger)\,|00\rangle\,, \end{aligned} \tag{34}$$

where the corresponding transmission and reflection coefficients are

$$t_k = \frac{1}{\sqrt{2}} \quad \text{and} \quad r_k = -\frac{\zeta_{2N}\zeta_N^k}{\sqrt{2}}. \tag{35}$$

The corresponding success probability is

$$p_{\text{succ}} = q^{2N}(1-q^2)^2\frac{2N!}{2^N}\frac{1}{N^N}. \tag{36}$$

In Fig. 4, the success probability is shown for various values of N. Further examples are presented in the appendices.

VII. EXPERIMENT

Based on the above theory, we also present an experiment on the generation of two-mode qutrit states ($n = 2$, $m = 2$). The experimental setup is shown in Fig. 5. This is a natural extension of a previous time-bin qubit experiment ($n = 1, m = 2$) [9]. Instead of preparing two independent nondegenerate optical parametric oscillators (NOPOs), we use a single NOPO, combined with two Mach-Zehnder interferometers on the idler side, with asymmetric arm lengths.

The NOPO, containing a periodically poled $KTiOPO_4$ crystal with a type-0 phase matching, is pumped continuously in a weak-pump regime, generating two-mode squeezed vacuum beams (signal and idler beams) continuously, which have finite correlation times determined by the bandwidth of the NOPO cavity (about 12 MHz of full width at half maximum). The signal and idler fields are two frequency modes of the NOPO cavity, separated by a free spectrum range (FSR) of about 600 MHz. An acousto-optic modulator (AOM) shifts the frequency of the pump beam by this FSR frequency, by which the signal field is at the frequency of local oscillators (LOs) for homodyne detections, while the idler field is at a different frequency separated by the FSR. As optical phase references, weak coherent beams are injected into the NOPO for both the

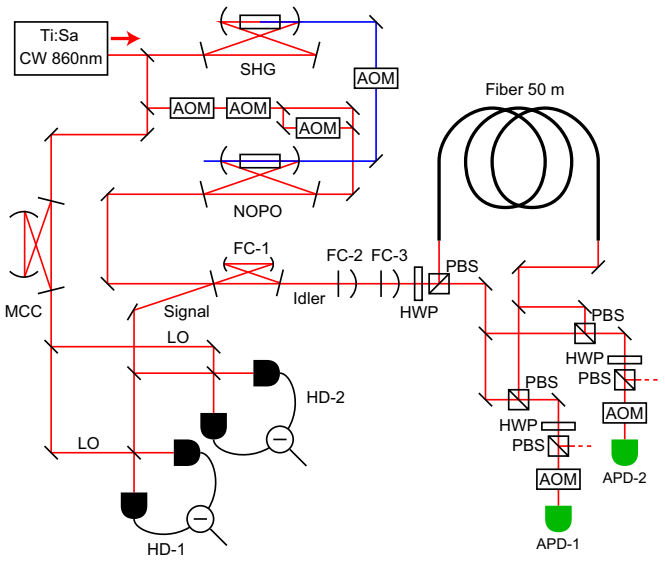

FIG. 5. Experimental setup. Ti:Sa denotes Ti:sapphire laser; CW: continuous wave; SHG: second harmonic generator; FC: filter cavity; MCC: spatial-mode cleaning cavity; and HD: homodyne detector.

signal and idler frequencies, which are switched on and off by AOMs. Feedback control of the optical system is performed by using the coherent beams, while qutrit states are generated when the coherent beams are absent.

The signal and idler fields are spatially separated by a filter cavity (FC-1 in Fig. 5) whose round-trip length is half of that of the NOPO. Additional two filter cavities (FC-2 and FC-3 in Fig. 5) further eliminate irrelevant fields before photon detections. After the filtering of the idler field, there are two Mach-Zehnder interferometers. The optical delay lines in the two Mach-Zehnder interferometers are common, implemented with a polarization-maintaining optical fiber with a length of about 50 m. Thanks to the delay line, sufficiently time-shifted idler fields interfere before the photon detection, which enables the heralded generation of time-bin superposition states. In order to control the transmission and reflection coefficients that determine the heralded state (see Appendix A), variable beam splitters are constructed with half-wave plates (HWPs) and polarization beam splitters (PBSs). The absolute values of the transmission and reflection coefficients are controlled by the angles of the wave plates, while the phases are feedback controlled using piezoactuated mirrors. The angles of the wave plates are adjusted by referring to the photon-counting rate from each arm.

When two silicone avalanche photodiodes (APDs) detect a photon simultaneously on the idler side, a qutrit state is heralded on the signal side. The idler field before each APD is coupled to a single-mode optical fiber for mode selection, and therefore there is no degradation of heralded states caused by imperfect interference visibilities of the Mach-Zehnder interferometers. AOMs before the APDs are switched on and off for protection of the APDs so that coherent phase-reference beams do not enter the APDs. We set a time window of about 30 ns to judge two photon detection events to be simultaneous. Simultaneous detection events were about 50 times per second. Note that the event rate is theoretically state dependent for the reasons discussed in Sec. III A, and we surely observed such dependence in the experiment (e.g., the event rate of generating $|2,0\rangle$ is twice as large as that of generating $|1,1\rangle$ with the same pumping power).

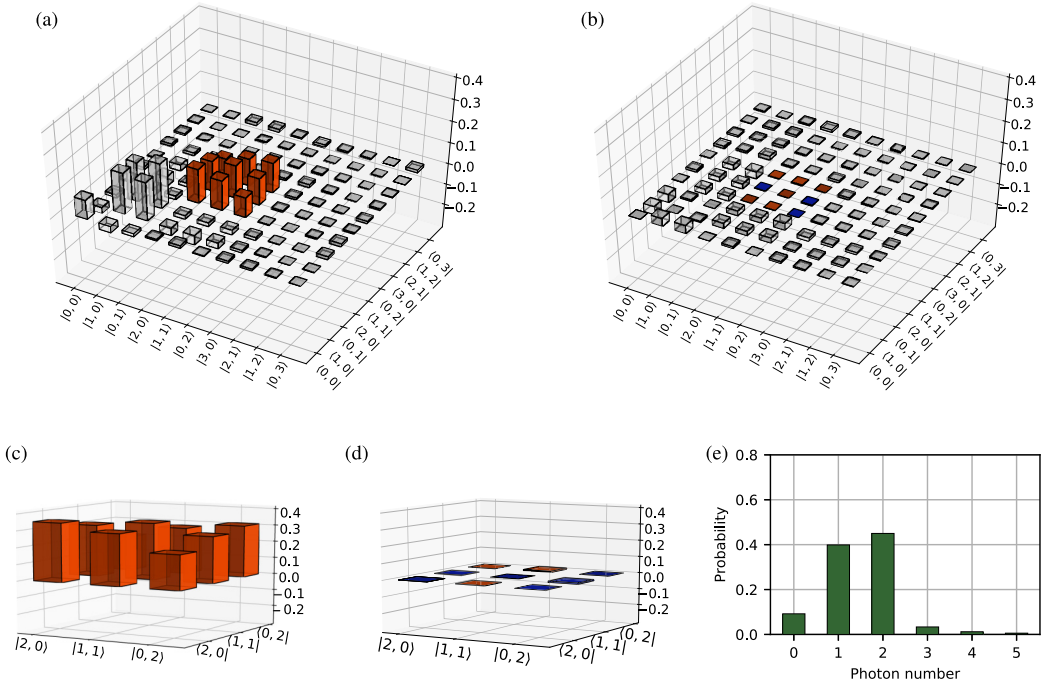

FIG. 6. Experimental density matrix for $(|2,0\rangle + |1,1\rangle + |0,2\rangle)/\sqrt{3}$. For the qutrit matrix elements, positive elements are colored in orange (light gray) and negative elements are colored in blue (gray). (a) Density matrix (real part), (b) Density matrix (imaginary part), (c) Qutrit subspace (real part), (d) Qutrit subspace (imaginary part), and (e) Probability of total photon number.

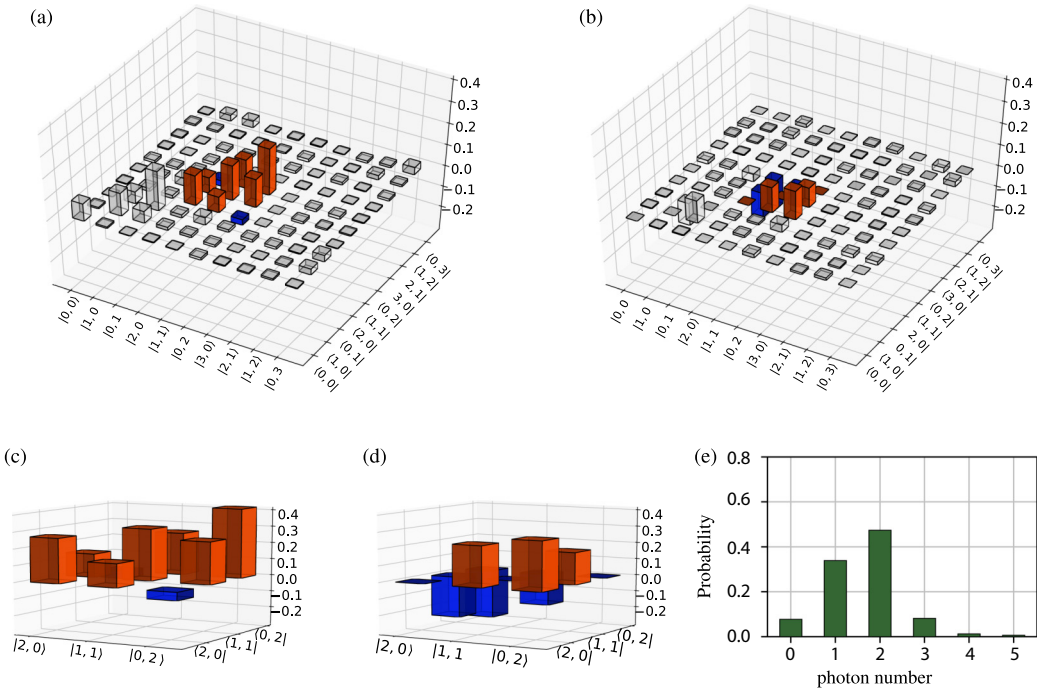

FIG. 7. Experimental density matrix for $[\sqrt{2}\,|2,0\rangle + (1+\sqrt{2}i)\,|1,1\rangle + 2i\,|0,2\rangle]/3$. For the qutrit matrix elements, positive elements are colored in orange (light gray) and negative elements are colored in blue (gray). (a) Density matrix (real part), (b) Density matrix (imaginary part), (c) Qutrit subspace (real part), (d) Qutrit subspace (imaginary part), and (e) Probability of total photon number.

The signal field, reflected by the first filter cavity, is sent to the characterization setup. The heralded state is, instead of photon-detection-based characterization [20], fully characterized with quantum tomography employing two homodyne detectors for simultaneous measurements of conjugate quadrature variables [9]. For each quantum state, quadrature values of 20 000 events were utilized for estimation.

Here we show the results of two qutrit states as examples. One state is $(|2,0\rangle + |1,1\rangle + |0,2\rangle)/\sqrt{3}$ and the other one is $[\sqrt{2}\,|2,0\rangle + (1+\sqrt{2}i)\,|1,1\rangle + 2i\,|0,2\rangle]/3$. The resulting density matrices are shown in Figs. 6 and 7, respectively. Real and imaginary parts of the density matrices are shown for both the full space up to three photons and the qutrit subspace. The distributions of the total photon number are calculated from the diagonal elements of Figs. 6(a) and 7(a), and shown in Figs. 6(e) and 7(e). The two-photon components, i.e., the probability of the state existing in the qutrit subspace, were 49% and 47%, respectively (constantly 45–50%), which are consistent with the heralded single-photon purity of about 70% (i.e., about 30% of losses). One-photon components as well as vacuum components are also consistent with the losses. These unwanted components will be suppressed by reducing optical losses in the signal line (known optical losses are 3% inside the NOPO and 3% in the transmission line after the NOPO), homodyne detection inefficiencies (mainly caused by mode mismatch with the LOs corresponding to interference visibilities of about 97%), and fake clicks from the APDs (estimated as about 1% from each APD). On the other hand, three-photon components which are less than 10% can be further suppressed by attenuating the pump power. The matrices for the qutrit subspace [Figs. 6(c), 6(d), 7(c), and 7(d)] are renormalized by the two-photon probability. The fidelities regarding the qutrit subspace were 93% and 95%, respectively (constantly over 90%). The fidelities will be improved if the precision and stability of our experimental setup are enhanced, such as the polarization in the fiber delay line.

VIII. CONCLUSION

We proposed a scheme to generate arbitrary qudit states in a heralded fashion, distributing n photons ($d = n + 1$) in two modes as a superposition state, based on two-mode squeezed states and photon detections. We further discussed an extension of our scheme to $m \geqslant 3$ modes, which may sometimes be possible, but not in general. Furthermore, we experimentally demonstrated our scheme by generating some exemplary qutrit states. States that can be created with our scheme include important states for quantum information applications, such as NOON states with $N \geqslant 3$ and encoded quantum error-correction states to suppress photon loss.

ACKNOWLEDGMENTS

This work was partly supported by CREST of JST, JSPS KAKENHI, and APSA, of Japan. P.v.L. and M.B. acknowledge support from Q.com (BMBF).

APPENDIX A: TWO-PHOTON STATES

Let us consider the balanced superposition $\frac{1}{\sqrt{3}}(|20\rangle + |02\rangle + |11\rangle)$, which cannot be obtained by linear optics alone.

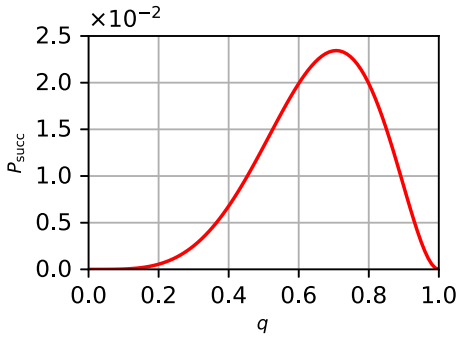

FIG. 8. Success probability for creating $\frac{1}{\sqrt{3}}(|20\rangle + |02\rangle + |11\rangle)$ in dependence of q (using photon-number-resolving detectors).

We can write

$$\begin{aligned}
&\frac{1}{\sqrt{3}}(|20\rangle + |02\rangle + |11\rangle)\\
&= \frac{1}{\sqrt{3}}\left(\frac{a_1^{\dagger 2}}{\sqrt{2}} + \frac{a_1^{\dagger 2}}{\sqrt{2}} + a_1^\dagger a_2^\dagger\right)|00\rangle\\
&= \sqrt{\frac{1}{6}}\left[a_1^\dagger + \frac{1}{\sqrt{2}}(1-i)a_2^\dagger\right]\left[a_1^\dagger + \frac{1}{\sqrt{2}}(1+i)a_2^\dagger\right]|00\rangle\\
&= \sqrt{\frac{2}{3}}\left[\frac{a_1^\dagger}{\sqrt{2}} + \frac{1}{2}(1-i)a_2^\dagger\right]\left[\frac{a_1^\dagger}{\sqrt{2}} + \frac{1}{2}(1+i)a_2^\dagger\right]|00\rangle\,.
\end{aligned} \tag{A1}$$

The probability for successful generation is thus $P_{\mathrm{succ}} = \frac{3}{8}q^4(1-q^2)^2$, which is plotted in Fig. 8.

A general superposition of two-photon states can be decomposed as follows:

$$\begin{aligned}
&\alpha\,|20\rangle + \beta\,|02\rangle + \gamma\,|11\rangle\\
&= \left(\frac{\alpha}{\sqrt{2}}a_1^{\dagger 2} + \frac{\beta}{\sqrt{2}}a_2^{\dagger 2} + \gamma a_1^\dagger a_2^\dagger\right)|00\rangle\\
&= \frac{\alpha}{\sqrt{2}}\left[a_1^\dagger - a_2^\dagger\left(-\frac{\gamma}{\sqrt{2}\alpha} + \sqrt{\frac{\gamma^2}{2\alpha^2} - \frac{\beta}{\alpha}}\right)\right]\\
&\quad\times\left[a_1^\dagger - a_2^\dagger\left(-\frac{\gamma}{\sqrt{2}\alpha} - \sqrt{\frac{\gamma^2}{2\alpha^2} - \frac{\beta}{\alpha}}\right)\right]|00\rangle\,.
\end{aligned} \tag{A2}$$

The corresponding transmission and reflection coefficients are

$$t_1 = \frac{1}{\sqrt{1 + \left|-\frac{\gamma}{\sqrt{2}\alpha} + \sqrt{\frac{\gamma^2}{2\alpha^2} - \frac{\beta}{\alpha}}\right|^2}}, \tag{A3a}$$

$$r_1 = \frac{-\frac{\gamma}{\sqrt{2}\alpha} + \sqrt{\frac{\gamma^2}{2\alpha^2} - \frac{\beta}{\alpha}}}{\sqrt{1 + \left|-\frac{\gamma}{\sqrt{2}\alpha} + \sqrt{\frac{\gamma^2}{2\alpha^2} - \frac{\beta}{\alpha}}\right|^2}} \tag{A3b}$$

$$t_2 = \frac{1}{\sqrt{1 + \left|\frac{\gamma}{\sqrt{2}\alpha} + \sqrt{\frac{\gamma^2}{2\alpha^2} - \frac{\beta}{\alpha}}\right|^2}}, \tag{A3c}$$

$$r_2 = -\frac{\frac{\gamma}{\sqrt{2}\alpha} + \sqrt{\frac{\gamma^2}{2\alpha^2} - \frac{\beta}{\alpha}}}{\sqrt{1 + \left|\frac{\gamma}{\sqrt{2}\alpha} + \sqrt{\frac{\gamma^2}{2\alpha^2} - \frac{\beta}{\alpha}}\right|^2}}. \tag{A3d}$$

APPENDIX B: THREE-MODE STATES

Using the methods described above, as an example of a three-mode state that can indeed be created, we present the following state:

$$\begin{aligned}
&\frac{1}{2\sqrt{3}}(a_1^\dagger + a_2^\dagger)(a_1^\dagger + a_3^\dagger)(a_2^\dagger - a_3^\dagger)\,|000\rangle\\
&= \frac{1}{2\sqrt{3}}(a_1^{\dagger 2}a_2^\dagger - a_1^{\dagger 2}a_3^\dagger - a_1^\dagger a_3^\dagger + a_2^{\dagger 2}a_1^\dagger + a_2^{\dagger 2}a_3^\dagger - a_3^{\dagger 2}a_2^\dagger)\,|000\rangle\\
&= \frac{1}{\sqrt{3}}\left(|2\rangle\,\frac{|10\rangle - |01\rangle}{\sqrt{2}} + |1\rangle\,\frac{|20\rangle - |02\rangle}{\sqrt{2}} + |0\rangle\,\frac{|21\rangle - |12\rangle}{\sqrt{2}}\right).
\end{aligned} \tag{B1}$$

[1] B. Yurke and D. Stoler, Generating Quantum Mechanical Superpositions of Macroscopically Distinguishable States Via Amplitude Dispersion, Phys. Rev. Lett. **57**, 13 (1986).

[2] R. L. Hudson, When is the Wigner quasi-probability density non-negative? Rep. Math. Phys. **6**, 249 (1974).

[3] A. I. Lvovsky, H. Hansen, T. Aichele, O. Benson, J. Mlynek, and S. Schiller, Quantum State Reconstruction of the Single-Photon Fock State, Phys. Rev. Lett. **87**, 050402 (2001).

[4] A. I. Lvovsky and J. Mlynek, Quantum-Optical Catalysis: Generating Nonclassical States of Light by Means of Linear Optics, Phys. Rev. Lett. **88**, 250401 (2002).

[5] E. Bimbard, N. Jain, A. MacRae, and A. I. Lvovsky, Quantum-optical state engineering up to the two-photon level, Nat. Photon. **4**, 243 (2010).

[6] M. Yukawa, K. Miyata, T. Mizuta, H. Yonezawa, P. Marek, R. Filip, and A. Furusawa, Generating superposition of up-to three photons for continuous variable quantum information processing, Opt. Express **21**, 5529 (2013).

[7] M. Yukawa, K. Miyata, H. Yonezawa, P. Marek, R. Filip, and A. Furusawa, Emulating quantum cubic nonlinearity, Phys. Rev. A **88**, 053816 (2013).

[8] A. Zavatta, M. D'Angelo, V. Parigi, and M. Bellini, Remote Preparation of Arbitrary Time-Encoded Single-Photon Ebits, Phys. Rev. Lett. **96**, 020502 (2006).

[9] S. Takeda, T. Mizuta, M. Fuwa, J. Yoshikawa, H. Yonezawa, and A. Furusawa, Generation and eight-port homodyne characterization of time-bin qubits for continuous-variable quantum information processing, Phys. Rev. A **87**, 043803 (2013).

[10] A. Ourjoumtsev, R. Tualle-Brouri, J. Laurat, and P. Grangier, Generating optical Schrödinger kittens for quantum information processing, Science **312**, 83 (2006).

[11] J. S. Neergaard-Nielsen, B. Melholt Nielsen, C. Hettich, K. Mølmer, and E. S. Polzik, Generation of a Superposition of Odd Photon Number States for Quantum Information Networks, Phys. Rev. Lett. **97**, 083604 (2006).

[12] K. Wakui, H. Takahashi, A. Furusawa, and M. Sasaki, Photon subtracted squeezed states generated with periodically poled $KTiOPO_4$, Opt. Express **15**, 3568 (2007).

[13] C. Guerlin, J. Bernu, S. Deléglise, C. Sayrin, S. Gleyzes, S. Kuhr, M. Brune, J.-M. Raimond, and S. Haroche, Progressive field-state collapse and quantum non-demolition photon counting, Nature (London) **448**, 889 (2007).

[14] I. L. Chuang, D. W. Leung, and Y. Yamamoto, Bosonic quantum codes for amplitude damping, Phys. Rev. A **56**, 1114 (1997).

[15] J. Yoshikawa, K. Makino, S. Kurata, P. van Loock, and A. Furusawa, Creation, Storage, and on-Demand Release of Optical Quantum States with a Negative Wigner Function, Phys. Rev. X **3**, 041028 (2013).

[16] E. Bimbard, R. Boddeda, N. Vitrant, A. Grankin, V. Parigi, J. Stanojevic, A. Ourjoumtsev, and P. Grangier, Homodyne Tomography of a Single Photon Retrieved on Demand from a Cavity-Enhanced Cold Atom Memory, Phys. Rev. Lett. **112**, 033601 (2014).

[17] Y.-H. Kim, R. Yu, S. P. Kulik, Y. Shih, and M. O. Scully, Delayed "Choice" Quantum Eraser, Phys. Rev. Lett. **84**, 1 (2000).

[18] L. M. Duan, M. D. Lukin, J. I. Cirac, and P. Zoller, Long-distance quantum communication with atomic ensembles and linear optics, Nature (London) **414**, 413 (2001).

[19] M. Bergmann and P. van Loock, Quantum error correction against photon loss using NOON states, Phys. Rev. A **94**, 012311 (2016).

[20] A. Kuzmich, I. A. Walmsley, and L. Mandel, Violation of a Bell-type inequality in the homodyne measurement of light in an Einstein-Podolsky-Rosen state, Phys. Rev. A **64**, 063804 (2001).